Expression of S100A9 in adamantinomatous craniopharyngioma and its association with wet keratin formation

CHUAN ZHAO[1,2*], WENXIN HU[1*], NING LUO[1], XINGFU WANG[3], DA LIN[4] and ZHIXIONG LIN[1]

[1]Department of Neurosurgery, Sanbo Brain Hospital; [2]Department of Neuro-oncology, Sanbo Brain Hospital, Capital Medical University, Beijing 100093; [3]Department of Pathology, The First Affiliated Hospital, Fujian Medical University, Fuzhou, Fujian 350004; [4]Department of Neurosurgery, Beijing Luhe Hospital, Capital Medical University, Beijing 101199, P.R. China

Received December 20, 2022; Accepted March 16, 2023

DOI: 10.3892/etm.2023.11981

Abstract. Wet keratin is a hallmark of adamantinomatous craniopharyngioma (ACP), which is frequently infiltrated by inflammatory cells. S100 calcium-binding protein A9 (S100A9) has been confirmed to play a decisive role in the development of inflammation. However, the relationship between wet keratin (keratin nodules) and S100A9 in ACP is poorly understood. The objective of the present study was to explore the expression of S100A9 in ACP and its association with wet keratin formation. Immunohistochemistry and immunofluorescence were used to detect the expression of S100A9, β-catenin and Ki67 in 46 cases of ACP. A total of three online databases were used to analyze S100A9 gene expression and protein data. The results revealed that S100A9 was primarily expressed in wet keratin and some intratumoral and peritumoral cells, and its expression in wet keratin was upregulated in the high inflammation group ($P=1.800x10^{-3}$). In addition, S100A9 was correlated with the degree of inflammation ($r=0.6$; $P=7.412x10^{-3}$) and the percentage of Ki67-positive cells ($r=0.37$; $P=1.000x10^{-2}$). In addition, a significant correlation was noted between the area of wet keratin and the degree of inflammation ($r=0.51$; $P=2.500x10^{-4}$). In conclusion, the present study showed that S100A9 was upregulated in ACP and may be closely associated with wet keratin formation and the infiltration of inflammatory cells in ACP.

Introduction

Craniopharyngioma (CP) is one type of epithelial tumor originating from embryonic remnants in the sellar region, which most commonly occur in individuals aged 5-14 and 50-74 years (1). Traditionally, CP can be divided into two subtypes: Adamantinomatous CP (ACP) and papillary CP (PCP). The latest World Health Organization classification criteria define ACP and PCP as different types (2). ACP is driven by somatic *CTNNB1* mutations, and histologically contains palisade-like basal epithelium, loosely aggregated stellate reticulum, cell clusters composed of cells with nucleo-cytoplasmic accumulation of β-catenin, nodules of anucleated ghost cells with brightly eosinophilic cytoplasm termed wet keratin, calcification, cholesterol clefts and other structures. In addition, high levels of cytokines and inflammatory markers are frequently discovered in the stroma of ACP (3,4).

The mechanism underlying the formation of the special pathological structures of ACP remains to be elucidated, including wet keratin and calcification. S100 calcium-binding protein A9 (S100A9) is a calmodulin that is closely associated with cellular proliferation, differentiation and apoptosis, and is abundant in inflammatory cells, such as neutrophils. Therefore, S100A9 has also been identified as a crucial inflammatory factor (5). S100A9 is also expressed in keratinocytes in certain skin inflammatory diseases, and is expressed and released by keratinocytes and activated leukocytes during inflammation and bodily injury (6,7). Several genes of the S100 family and proteins involved in epidermal keratinization form the so-called epidermal differentiation complex on human chromosome 1q21 (8), and evidence has suggested that S100A9 is closely associated with epithelial differentiation (9). In view of the complex inflammatory microenvironment of ACP, it was hypothesized that epithelial differentiation associated with S100A9 may be involved in the formation of wet keratin. Therefore, the present study investigated the expression of S100A9 in ACP and its association with wet keratin formation, in order to obtain improved insight into the tumor biology of ACP.

Materials and methods

Demographic and clinical data. All sample tissues were obtained from cases that underwent surgery (including radical resection and conservative resection) at Beijing Sanbo Brain Hospital (Beijing, China) between September 2016 and September 2019. Cases were selected that had complete

Correspondence to: Professor Zhixiong Lin, Department of Neurosurgery, Sanbo Brain Hospital, Capital Medical University, 50 Yikesong Road, Xiangshan, Haidian, Beijing 100093, P.R. China
E-mail: linzx@ccmu.edu.cn

*Contributed equally

Key words: adamantinomatous craniopharyngioma, S100 calcium-binding protein A9, Ki67, wet keratin, inflammation

clinical information and histological specimens, and for whom follow-up data could be obtained. Cases were excluded that did not have complete clinical information or enough histological specimens, or follow-up data could not be obtained. A total of 46 eligible cases were included in the present study. The baseline data were collected, including age, sex, radiological images, surgical resection and postoperative recurrence (Table I). Follow-up ended in March 2022, and tumor recurrence or death was considered a progressive event. The patients in the present study provided written informed consent. The present study was designed in accordance with The Declaration of Helsinki and approved by the ethics committee of Sanbo Brain Hospital, Capital Medical University (Beijing, China; ethical approval no. SBNK-YJ-2020-014-01).

Table I. Baseline data of patients.

Factor	Values
Sex	
Male	33
Female	13
Age, years, median (IQR)	11.38 (13.06)
Consistency	
Predominantly cystic	29
Predominantly solid	17
Preoperative status	
Primary	16
Recurrent	30
Resection	
Radical resection	42
Conservative resection	4
Postoperative status	
Recurrence	7
No recurrence	39

Hematoxylin and eosin (H&E) staining. Following surgery, the tissue specimens were immersed in 10% formalin for 24-48 h at room temperature. Then the tissue specimens were placed into molds supplemented with liquid paraffin, cooled and frozen to make the paraffin solid to achieve tissue fixation, and sectioned using a paraffin microtome. The wax blocks were cut into 4-μm sections for H&E staining. Sections were stained with hematoxylin for 0.5-1 min, rinsed with running water, differentiated in 1% hydrochloric acid alcohol for a few seconds, rinsed with running water, then returned to 1% ammonia aqueous solution for 1 min, rinsed with running water for a few seconds, stained in eosin staining solution for a few seconds and sealed after rinsing with running water. All the above experimental procedures were carried out at room temperature. Light field microscopy was used for observation.

Immunohistochemistry and immunofluorescence. Following fixation in 10% formalin for 24-48 h at room temperature, the samples were dehydrated in increasing ethanol concentrations, then samples were embedded in paraffin, the wax blocks were cut into 4-μm sections, deparaffinized in xylene and rehydrated with graded ethanol. Antigen retrieval was performed using Tris-EDTA buffer (pH 9.0) in a 95˚C water bath for 15 min. Endogenous peroxidase was inactivated with 3% H_2O_2 for 10 min at room temperature. and samples were washed with phosphate-buffered saline (PBS). After blocking using the peroxidase blocking agent for 15 min at room temperature, the sections were incubated with the primary antibody overnight at 4˚C and then rinsed with PBS. Horseradish peroxidase-conjugated secondary antibody was added dropwise and incubated at 37˚C for 30 min and then rinsed with PBS. Samples were placed in diaminobenzidine and rinsed with PBS, and the slides were dehydrated, dried and sealed. Light field microscope was used for observation.

For double immunofluorescence staining, sections (prepared as for immunohistochemistry and immunofluorescence) were subjected to antigen retrieval using Tris-EDTA buffer (pH 9.0) in a 95˚C water bath for 20 min, and were then incubated with immunostaining blocking solution containing 0.1% Triton X-100 for 90 min at room temperature, The diluted primary antibody was then added to the slides and incubated overnight at 4˚C, before being rinsed with PBS containing 0.1% Triton X-100. The diluted fluorescence secondary antibody was added and incubated with the slides for 90 min at room temperature, before being rinsed with PBS containing 0.1% Triton X-100 and incubated with DAPI for 10 min. Immunofluorescence was assessed using a Leica fluorescence microscope (THUNDER Imager Tissue; Leica Microsystems, Inc.) and image analysis was performed using Leica Application suite X software (v3.1.5, Leica Microsystems, Inc.).

The primary antibodies used were S100A9 (Abcam; 1:400; ab92507), Ki67 (OriGene Technologies, Inc.; 1:200; cat. no. ZM-0167) and β-catenin (MAX; 1:200; cat. no. MAB-0754), and the secondary antibodies were conjugated to Alexa Fluor 488 (Abcam; 1:500; cat. no. ab150077) or 647 (Abcam; 1:500; cat. no. ab150115).

Specimen evaluation. Antibody expression was evaluated by two observers and supervised by an experienced pathologist. Tissue samples were divided by H&E staining into a high-inflammation group and a low-inflammation group, according to the degree of inflammatory cell infiltration. Tissues with extensive aggregation of inflammatory cells were included in the high-inflammation group and tissues with scattered distribution of inflammatory cells were included in the low-inflammation group. To assess the degree of inflammation, five areas containing inflammatory cells in the field of vision that could be observed and counted were selected and the percentage of inflammatory cells was counted. For Ki67 staining, brown nuclei were regarded as positive, and five dense areas of positive cells were randomly selected to count the number of positive cells, and the percentage of positive cells was calculated as previously described (10). Expression of S100A9 was evaluated in wet keratin, with brown tissue considered positive; according to the degree of staining, the tissue was classified as strongly positive (3 points), moderately positive (2 points) and weakly positive (1 point) (11). A total of five fields of vision were randomly selected, and the percentage of S100A9-positive areas

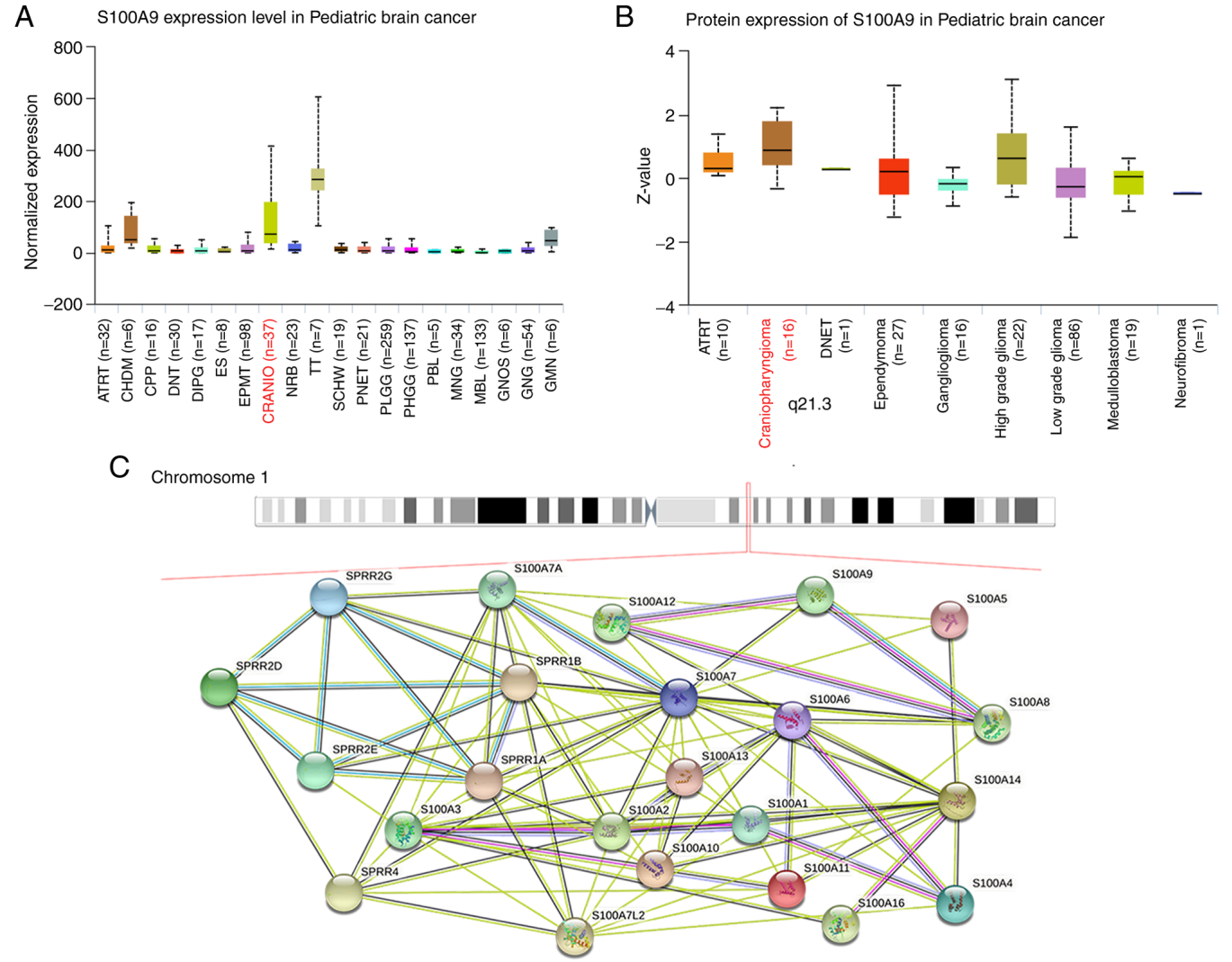

Figure 1. Online databases validate the expression of S100A9 in craniopharyngioma. (A) mRNA expression of S100A9 in pediatric brain tumors. (B) Protein expression of S100A9 in pediatric brain tumors. (C) The S100A9 gene located on chromosome 1q21.3 involved in the formation of epidermal differentiation complex had complex protein-protein interactions with epidermis-related SPRR genes and S100A family genes. S100A9, S100 calcium-binding protein A9; SPRR, small proline-rich protein.

were estimated for each field; finally, the S100A9 scores of each case were calculated, score=∑ (S100A9 percentage x degree of staining)/5, as previously described (12,13). The percentage of areas of wet keratin was also counted via H&E staining to analyze the relationship between wet keratin and inflammation.

Online databases. The chromosomal location of the S100A9 gene was determined from the Ensembl database (http://www.ensembl.org; release 109). The protein-protein interaction was analyzed by STRING (https://cn.string-db.org/). RNA and protein data were obtained from the pediatric brain tumor online database (The University of Alabama at Birmingham Cancer data analysis portal; Pediatric brain cancer in CBTTC dataset: https://ualcan.path.uab.edu/cgi-bin/CBTTC-Result.pl?genenam=S100A9); RNA and protein data from various pediatric brain tumors, including ACP, were used to assess the RNA and protein expression levels of S100A9.

Data analysis. R (v4.1.1 https://mirrors.tuna.tsinghua.edu.cn/CRAN/) and GraphPad Prism (v8.0; GraphPad Software; Dotmatics) were used for statistical analysis. Measurement data are shown as the mean ± standard deviation and median (IQR), normally distributed data were assessed using the two-sample unpaired t-test and non-normally distributed data (age comparison of S100A9 high group and low group) were assessed using the Mann-Whitney U test. The χ^2 test was used for contingency tables. A linear correlation analysis was performed using Spearman's test. Survival analysis was performed using the Kaplan-Meier test and log-rank test. $P<0.05$ was considered to indicate a statistically significant difference.

Results

Online databases validate the expression of S100A9 in ACP. Online databases were used to verify the RNA and protein expression levels of S100A9 in ACP. The RNA expression of S100A9 ranked second in ACP among all detected pediatric brain tumors, after teratoma. Protein expression was ranked first (Fig. 1A and B). Several genes of the S100 family and proteins involved in epidermal cornification

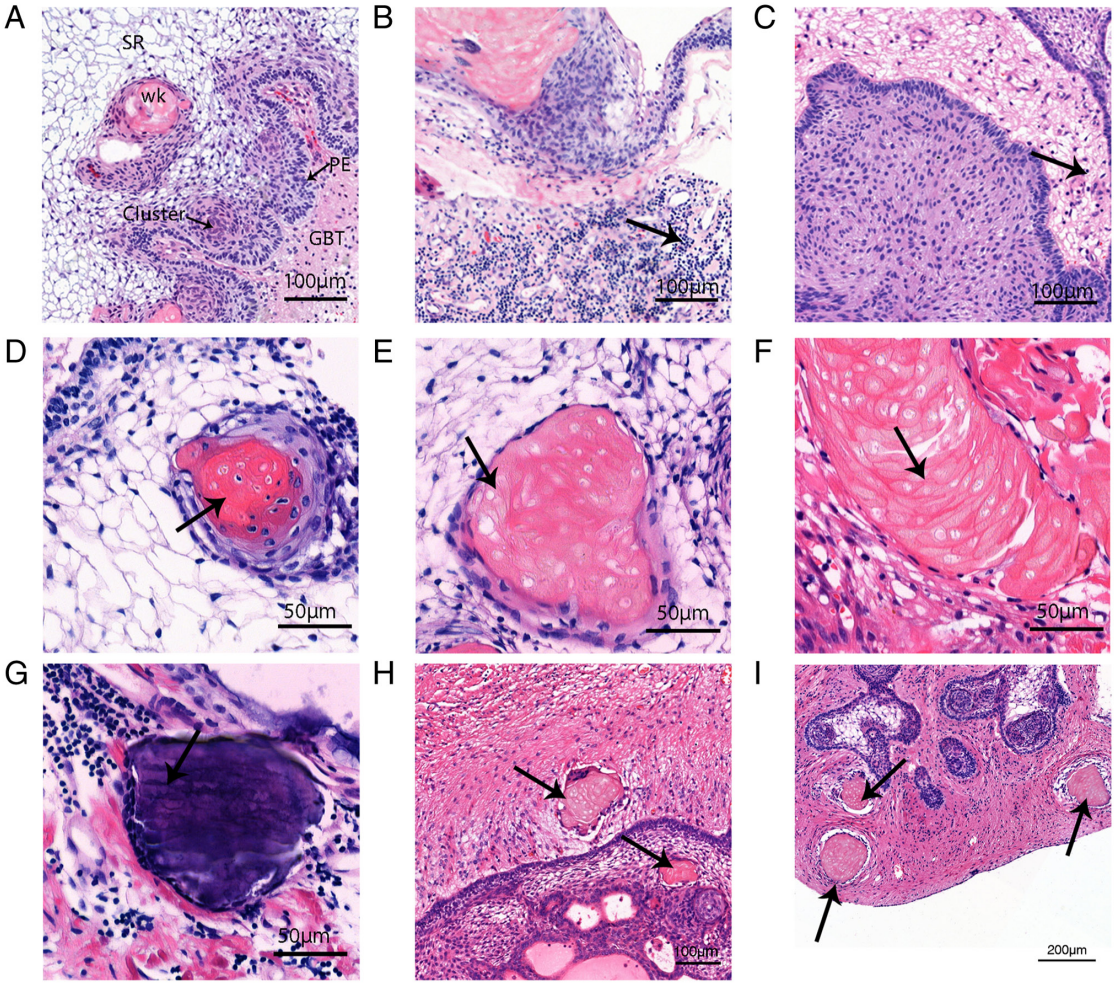

Figure 2. Stepwise evolution of wet keratin in ACP. (A) The pathological structure of ACP. (B) Inflammatory cells were extensively aggregated in the ACP high-inflammation group (arrow). (C) In the ACP low-inflammation group, distribution of inflammatory cells was scattered (arrow). (D) The wet keratin-like tumor cells gradually formed wet keratin and their nuclei gradually became smaller (arrow). (E) Wet keratin was formed, the nuclei disappeared and a cavity was then formed (arrow). (F) The wet keratin content increased, and layered and fused together to form a flaky area (arrow). (G) Clear blue calcium salt deposits appeared on wet keratin (arrow). (H) Wet keratin appeared in the invasive margin of the tumor and in the surrounding brain tissue and formed an isolated island shape (arrow). (I) Multiple wet keratins infiltrated into the surrounding brain tissue. ACP, adamantinomatous craniopharyngioma; wk, wet keratin; cluster, cells with nucleocytoplasmic accumulation of β-catenin; SR, stellate reticulum; PE, palisade-like basal epithelium; GBT, gliotic brain tissue.

form a so-called epidermal differentiation complex on human chromosome 1q21 (8). The protein-protein interaction between epidermis-related small proline-rich protein genes and S100A family genes was found in the adjacent chromosome location, showing a complex interaction between them (Fig. 1C). These data showed that S100A9 was indeed highly expressed in ACP and played an important role in tumorigenesis.

Inflammatory infiltration and wet keratin evolution detected using H&E staining. The typical pathological structures of ACP are shown in Fig. 2A. Extensive aggregation of inflammatory cells was observed in the high-inflammation group (Fig. 2B), and scattered distribution of inflammatory cells was observed in the low-inflammation group (Fig. 2C). The continuous evolutionary process from tumor cells to wet keratin was observed by H&E staining (Fig. 2D-F). Some tumor cells underwent apoptosis and nucleolysis, and all cells exhibited eosinophilic properties. The dissolved cellular components also fused and eventually calcium deposits appeared, suggesting that wet keratin evolved from dead tumor cells and the calcifications in ACP were the result of calcium salt deposition after wet keratin formation. Additionally, scattered isolated islands of wet keratin were seen in brain tissue (Fig. 2H and I).

Relationship between S100A9 and keratinization. Clusters with nucleocytoplasmic accumulation of β-catenin is characteristic of ACP. Clusters were shown by immunohistochemical staining but wet keratin was negative for β-catenin (Fig. 3A-C; derived from the same sample). Immunohistochemical results showed no obvious dark brown staining of wet keratin on the negative control (ACP tissue without S100A9 antibody) images (Fig. 3D). On the sections stained with the S100A9 antibody, the results showed that S100A9 was expressed in the wet keratin (Fig. 3E and I) and stellate reticulum (Fig. 3G). Some cells in clusters also showed weak positive expression (Fig. 3H) and S100A9 was highly expressed in the tumor stroma (Fig. 3F). In the basal palisades epithelium, S100A9 was partly expressed (Fig. 3H). S100A9 was also highly expressed in wet keratin (Fig. 3I). Immunofluorescence staining

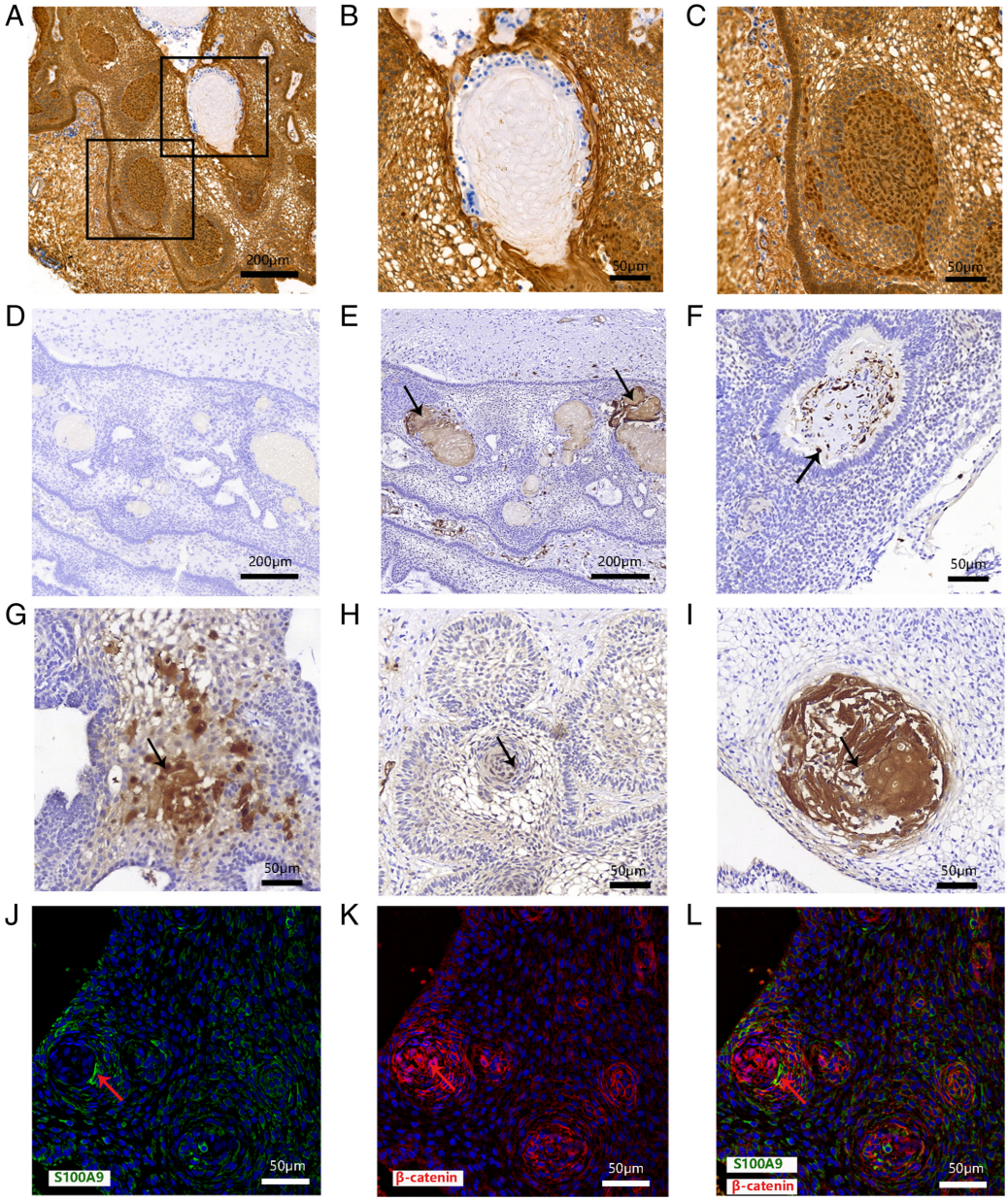

Figure 3. S100A9 is expressed in ACP. (A) Immunohistochemistry of β-catenin on ACP. (B) β-catenin staining for wet keratin was negative. (C) The cell cluster had nucleocytoplasmic accumulation of β-catenin. Fig. 3A-C are derived from the same sample. (D) No obvious dark brown staining of wet keratin was found in the negative control images. (E) S100A9 expression was positive in wet keratin (arrow; x5 objective). (F) S100A9 was expressed in the stroma surrounding the tumor (arrow). (G) S100A9 was partially expressed in stellate reticulum (arrow). (H) S100A9 showed weak positive staining in whorl-like cells in some cases (arrow). (I) S100A9 expression was positive in wet keratin (arrow; x20 objective) (J) Immunofluorescence staining showed that S100A9 was expressed on ACP tumor cells (green; red arrow). (K) β-catenin staining was nuclear positive in ACP cell cluster (red; arrow). (L) The merge of S100A9 and β-catenin showed that S100A9 was expressed around and inside whorl-like tumor cells (green; red arrow). ACP, adamantinomatous craniopharyngioma; S100A9, S100 calcium-binding protein A9.

showed that S100A9 was expressed in some ACP tumor cells positive for β-catenin. These results indicated that S100A9 was expressed in ACP intratumoral and extratumoral cells, especially in wet keratin (Fig. 3J-L).

Association between S100A9 and wet keratin. S100A9 was expressed in ACP cells, which were eosinophilic in H&E staining (Fig. 4A), and their morphology was from a bulk of normal tumor cells to a shape similar to wet keratin. S100A9 was also expressed in cells are in the process of transitioning from tumor cells to wet keratin (Fig. 4B-F). H&E staining and immunofluorescence showed island-like structures formed by S100A9-positive wet keratin invaded brain tissue around the tumor (Fig. 4G and H; Fig. 2H, upper arrow and Fig. 2I, arrows).

Association between S100A9 in wet keratin and inflammation. Scattered S100A9-positive cells were seen in the brain tissue outside the tumor and these cells became increasingly sparse in areas most distant from the tumor, which was similar to the degree of inflammation produced by the tumor stimulating the brain tissue (Fig. 5A and B). S100A9 was also distributed near the cholesterol cleft, where a large number of inflammatory cells also accumulated (Fig. 5C and D). Areas of

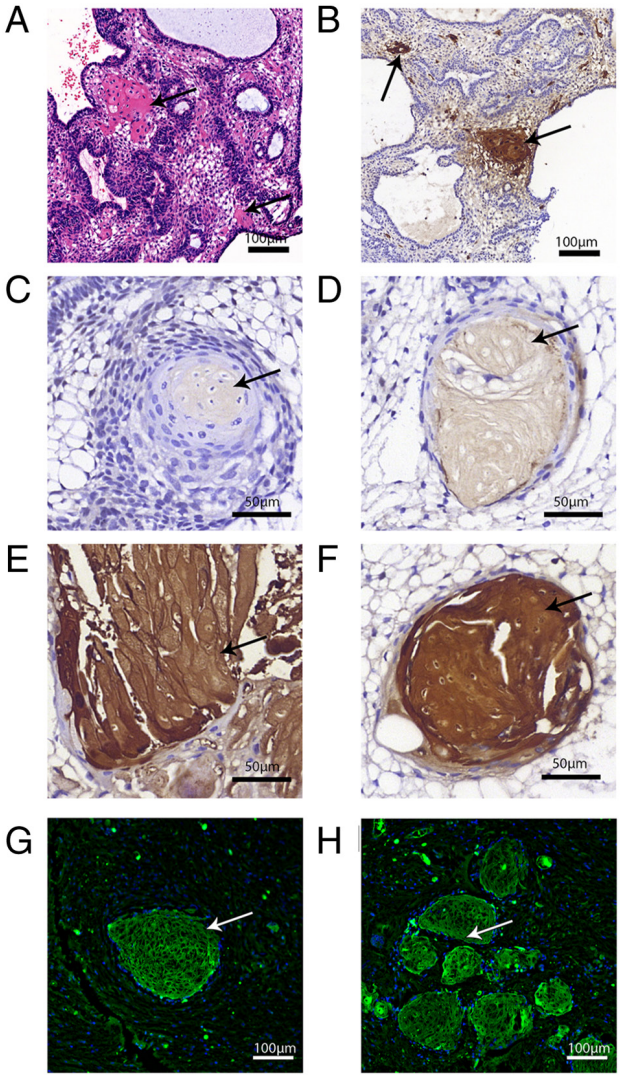

Figure 4. Wet keratin-like cells in H&E staining and wet keratin in immunostaining. (A) Wet keratin-like cells in H&E-stained tumor cells with eosinophilic features (arrow). (B) Patchy S100A9-positive areas in tumor cells, corresponding to H&E-stained wet keratin-like tumor cells (arrow). (C) The transitional morphology of tumor cells to wet keratin; the nucleus shrank and the cytolysis expanded (arrow). (D) Wet keratin was further formed, the nucleus shrank further into dark brown spots, and S100A9 staining intensified (arrow). (E) The previously shrunken nuclei disappeared, and the wet keratin area was larger, with some modules layered in long strips and fused with each other (arrow). (F) Circular stained area of wet keratin. (G) Immunofluorescence staining showed that a single S100A9-positive wet keratin infiltrated into the brain tissue surrounding the tumor (arrow). (H) Multiple S100A9-positive wet keratins infiltrated into the brain tissue surrounding the tumor (arrow). H&E, hematoxylin and eosin; S100A9, S100 calcium-binding protein A9.

wet keratin and the expression of S100A9 in wet keratin was correlated with inflammation in ACP (Fig. 5G and H). The scores of S100A9 in the group with higher inflammation were higher than those in the tumor group with lower inflammation, and the difference was statistically significant (Fig. 5I). The expression difference of S100A9 in the two groups is shown visually in Fig. 5E and F.

Association between S100A9 in wet keratin and proliferation. A number of studies have reported that S100A9 promotes cell proliferation, and inflammation is also an important factor in causing proliferation. No Ki67-positive cells were identified in wet keratin itself, but positive cells were found in scattered regions around wet keratin (Fig. 6A and B). An obvious linear correlation was found between S100A9 scores and percentage of Ki67-positive cells (Fig. 6C).

Association between the expression levels of S100A9 and various clinical factors. The baseline data of patients are shown in Table I. Patients were divided into two groups according to S100A9 score with the median as the cut-off. When the relationships between the expression levels of S100A9 and sex, age, tumor composition, preoperative status, resection and postoperative status were studied, no significant associations were found between S100A9 and various clinical factors (Table II). However, an association between S100A9 and recurrence-free survival was shown, and patients with high S100A9 expression had a poorer prognosis (Fig. 6D). But there was no significant difference between S100A9-High and S100A9-Low.

Discussion

In the present study, S100A9 was expressed in some tumor cells and wet keratin. Wet keratin labeled with S100A9 was also hypothesized to be involved in the evolution of keratin. According to the results of the present study, it can be hypothesized that tumor cells expressing S100A9 eventually evolve into wet keratin in ACP.

Wet keratin is a characteristic pathological structure of ACP, but its origin is unclear. Similar structures have been found in calcified odontogenic cysts, an odontogenic tumor histologically similar to ACP (14). Although no direct *in vitro* experimental study of cell evolution is available, the present study found the evolutionary process of wet keratin was traceable from histological and pathological morphological changes in wet keratin and is associated with ACP stem cell-like cells (15). Therefore, the present study inferred that the evolution of wet keratin was based on the morphological changes in wet keratin. Finally, after the formation of wet keratin, the corresponding metabolic and necrotic substances are deposited; for example, broken organelles, chromatin fragments, proteins and wet keratin deposited these substances may cause non-specific inflammation.

Previous studies have reported that the gene encoding epidermal keratinocyte structural protein and S100 calcium-binding protein form a gene complex ('epidermal differentiation complex') on human chromosome 1q21 (8,9). This suggested that S100 calcium-binding proteins are involved in keratinization. The present study also showed that S100A family members have complex interactions with adjacent epidermal differentiation genes.

It is well known that ACP is derived from residual embryonic tissue, which is homologous to the oral epithelium and is a typical epithelial tissue (1). The reason for the presence of wet keratin components in epithelial tumors remains to be elucidated. However, from the results of the present study, it is likely that S100A9 is closely associated with keratinization of cells in ACP to eventually form wet keratin. Wet keratin is common in human ACP but absent in the mouse model of ACP (16,17). Notably, the genomes of mice and rats lack

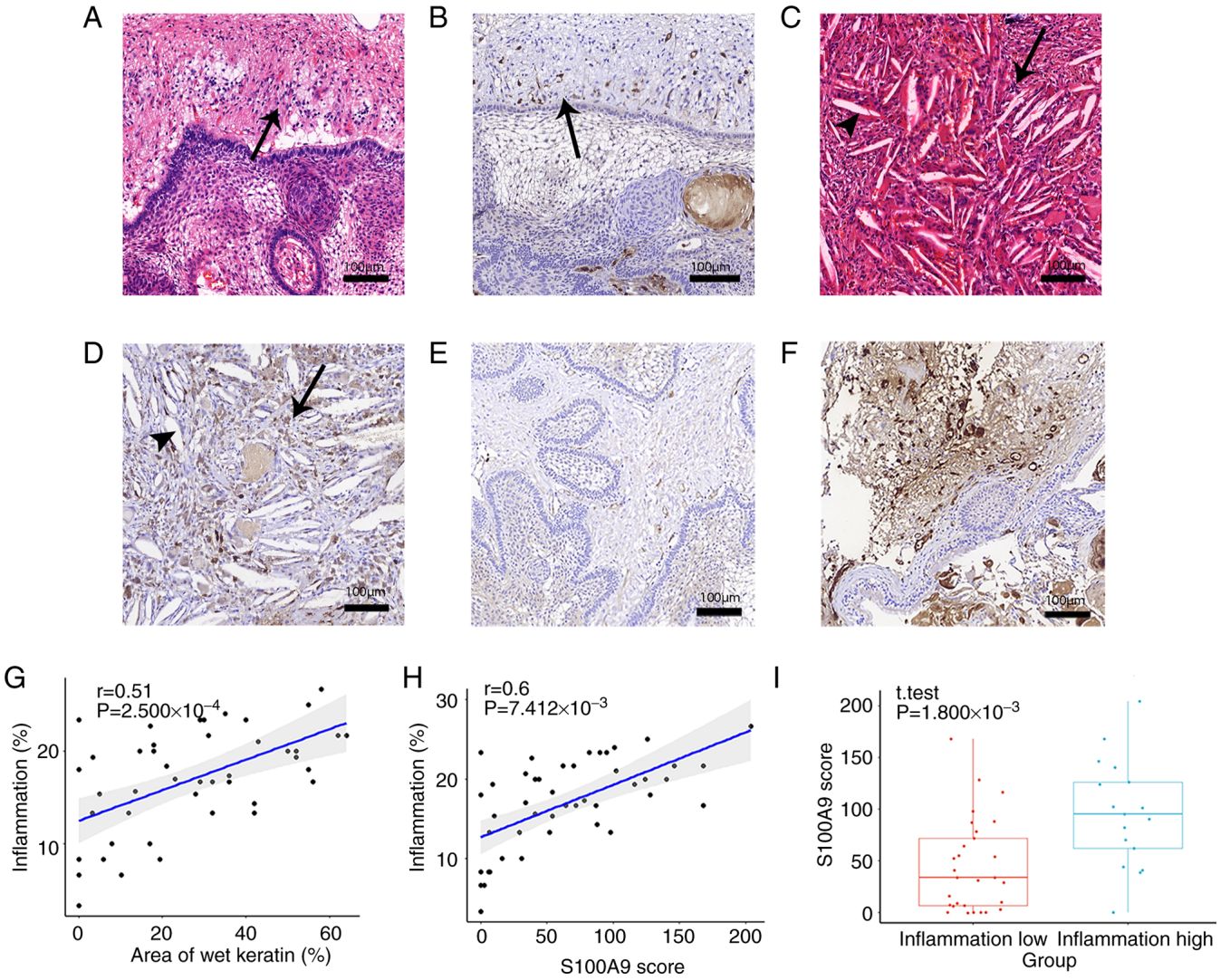

Figure 5. Wet keratin, S100A9 and inflammation. (A) H&E staining showed inflammatory cells (arrows) in the brain tissue surrounding the tumor margin. (B) Immunohistochemistry showed S100A9-positive areas (arrow) in brain tissue adjacent to the tumor. (C) H&E staining showed cholesterol clefts (arrowhead) surrounded by massive inflammatory cell infiltration (arrow). (D) Immunohistochemistry showed cholesterol clefts (arrowhead) surrounding evident S100A9 expression. (E) No or weak expression of S100A9 was observed in the intratumor and stroma of tumors in the low-inflammatory tumor group. (F) Strong expression of S100A9 was observed in both intratumor and stroma of tumors in the high-inflammatory tumor group. (G) The area of wet keratin was positively correlated with ACP inflammation ($P=2.500x10^{-4}$). (H) S100A9 expression in wet keratin was positively correlated with inflammation in ACP ($P=7.412x10^{-3}$). (I) Comparison of the S100A9 expression scores in the high-inflammation group and the low-inflammation group, with significantly higher S100A9 scores in the high inflammation group ($P=1.800x10^{-3}$, t-test). S100A9, S100 calcium-binding protein A9; H&E, hematoxylin and eosin; ACP, adamantinomatous craniopharyngioma.

S100A2, S100A12 and two members of the S100A family genes (18,19), This may be the potential biological basis for the lack of wet keratin in the mouse ACP model and not just a coincidence. In addition, S100A family members are calcium ion regulatory proteins (18), which, unsurprisingly, are suspected to be involved in the formation of calcification in ACP.

Enhanced inflammation in the tumor component of ACP is a hallmark of ACP (20-23). Various immune cells, including lymphocytes and myeloid-derived cells, are present in the immune microenvironment in ACP (10,24). Neutrophils contain abundant S100A9, which serves an important role in neutrophil N1-type polarization (25,26), thus S100A9-positive cells in intratumoral and peritumoral brain tissue may include ACP tumor-associated neutrophils. Accordingly, the present study could be the first definitive report on neutrophils in ACP, to the best of the authors' knowledge.

The brain tissue adjacent to the tumor is often infiltrated by inflammatory cells due to the mechanical stimulation of tumor growth and the possible stimulation of biochemical secretions (20). A large number of inflammatory cells has also been shown to infiltrate into the region of cholesterol crystals (20). On the whole, the severity of inflammation was consistent with the overall distribution of S100A9 and wet keratin observed in the present study. The results of the present study also showed that groups with a higher degree of inflammatory infiltration had higher S100A9 expression; in addition, both wet keratin and S100A9 were found to have a significant linear association with inflammation. These results demonstrated a close relationship between inflammation in ACP and both wet keratin and S100A9. S100A9 has also been reported to act through Toll-like receptor 4 and initiates the downstream inflammatory pathway, which is evidently

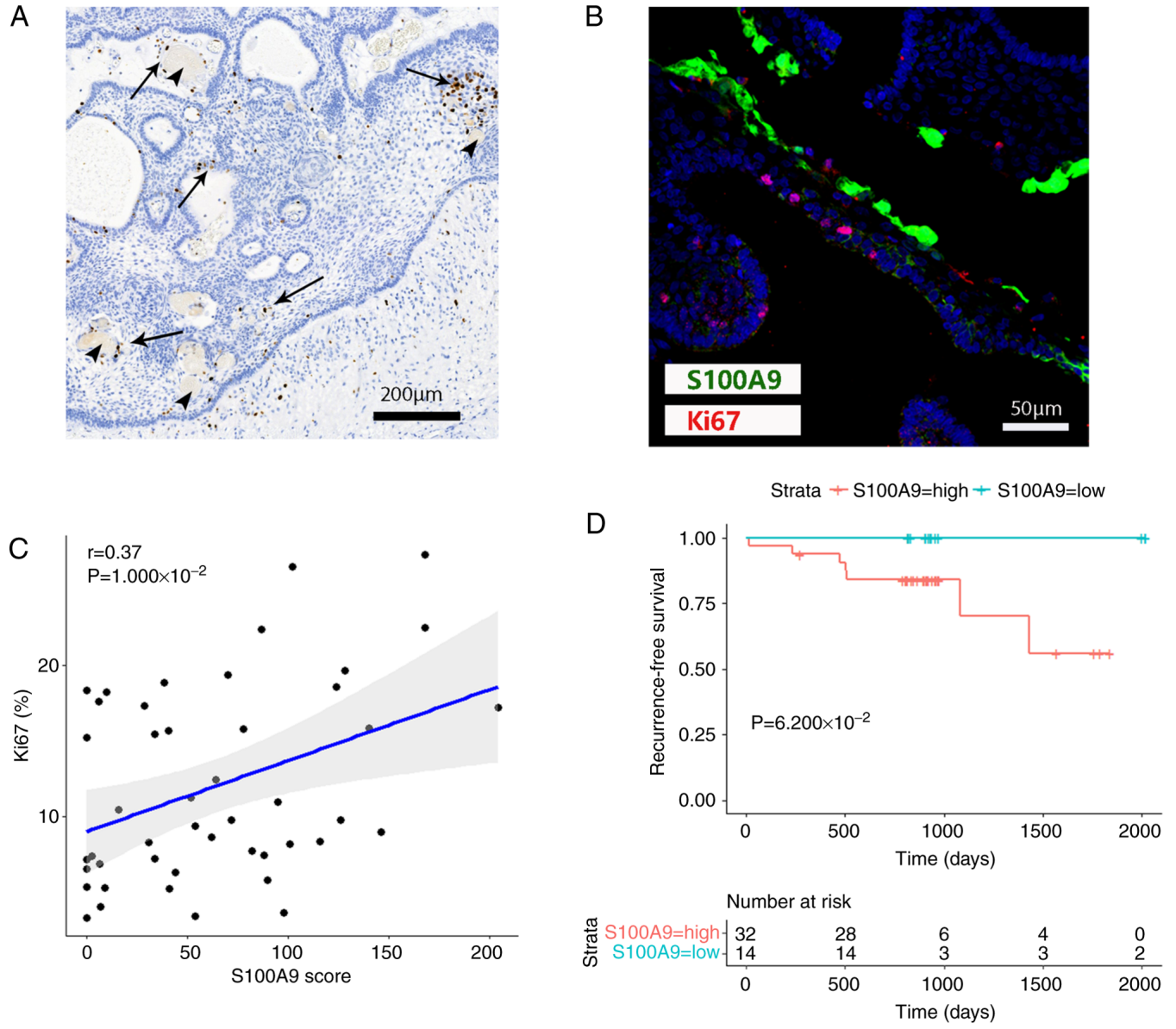

Figure 6. S100A9, Ki67 and prognosis. (A) Immunohistochemical staining for Ki67 showed no positive cells in the wet keratin area, but positive cells were found in scattered areas within the tumor and around the wet keratin (arrow, wet keratin; arrowhead, Ki67). (B) Immunofluorescence co-staining of S100A9 and Ki67. (C) A clear linear relationship was observed between S100A9 scores and the percentage of Ki67-positive cells ($P=1.000x10^{-2}$). (D) S100A9 showed a trend of influencing recurrence-free survival of patients ($P=6.200x10^{-2}$). S100A9, S100 calcium-binding protein A9.

associated with immunity and inflammation (27,28). S100A9 also serves an important role in inflammation of multiple organs and cancer (29,30). The results of the present study are consistent with those of previous studies, showing that S100A9 appears to be a crucial molecule during the inflammatory process of ACP.

The present study also showed a linear correlation between S100A9 and tumor cell proliferation. A previous study showed that S100A family members promote tumor proliferation, and some researchers have used it as a potential target for therapy (31). In the present study, the expression of S100A9 was significantly and linearly correlated with Ki67, reflecting that S100A9 may promote the proliferation of ACP. Notably, S100A9 acts as an inflammation-related factor before tumor metastasis and is associated with tumor metastasis, which suggests that the expression pattern of S100A9 in tumor parenchyma in ACP and the invasiveness of ACP deserve further study (32,33). It is worth mentioning that the present study also found that wet keratin can transcend the tumor boundary and enter the surrounding structures to form island-like structures, which may be a mode of invasive growth of ACP. Given the critical role of S100A9 in ACP related to inflammation, proliferation and metastasis, therapy with drugs such as Tasquinimod or Paquinimod may be a promising direction.

While the present study expanded the understanding of the mechanism underlying wet keratin and its relationship with inflammation in ACP, evidence is still lacking. S100A9 is associated with inflammation in ACP. A limitation of the present study was that it did not have live ACP cells and functional assays related to S100A9 could not be performed, thus the present study lacked evidence of S100A9 interaction

Table II. Association between S100A9 scores and clinical factors.

	S100A9 scores		
Clinical factors	≤54	>54	P-value
Sex			$6.079x10^{-1}$
Male	18	15	
Female	6	7	
Age, years, median (IQR)	11.96 (21.63)	11.08 (7.89)	$6.589x10^{-1}$
Consistency			$5.949x10^{-1}$
Predominantly cystic	16	13	
Predominantly solid	8	9	
Preoperative status			$1.457x10^{-1}$
Primary	6	10	
Recurrent	18	12	
Resection			$9.274x10^{-1}$
Radical resection	22	20	
Conservative resection	2	2	
Postoperative status			$7.750x10^{-1}$
Recurrence	4	3	
No recurrence	20	19	

The median of the S100A9 score was 54. S100A9, S100 calcium-binding protein A9.

with inflammatory cells and it was not possible to prove that S100A9 causes inflammation in ACP. The role played by the S100 protein family in primary tumors and metastases remains to be elucidated and needs further exploration.

The function of S100A9 in ACP may be further demonstrated by animal studies. At the same time, unlike human craniopharyngioma, wet keratin has not been found in mouse models of craniopharyngioma, which some researchers attribute to species differences, but evidence is still insufficient (34). Whether S100A family members are responsible for this difference may be revealed in future studies.

The present study found that wet keratin evolved from some tumor cells in ACP and these tumor cells expressed S100A9. It was hypothesized that S100A9 was involved in the evolution of wet keratin, and S100A9 was associated with inflammation in ACP.

Acknowledgements

The authors would like to thank Mr. Zhong Ma (Sanbo Brain Hospital, Capital Medical University, Beijing, China), for his excellent assistance.

Funding

The present study was supported by grants from Sanbo Brain Hospital Management Group (grant no. SBJT-KY-2020-002) and Capital's Funds for Health Improvement and Research (grant no. 2022-2-8013).

Availability of data and materials

The datasets used and/or analyzed during the current study are available from the corresponding author on reasonable request.

Authors' contributions

ZL conceived and designed the current study. All authors participated in the acquisition of data. Analysis and interpretation of data was performed by CZ, WH, DL, NL and XW. CZ and ZL drafted the manuscript. XW and ZL critically revised the manuscript. ZL reviewed the submitted version of manuscript and approved the final version of the manuscript on behalf of all authors. CZ and XW performed statistical analysis. Administrative, technical and material support was from ZL who also supervised the study. WH and ZL confirm the authenticity of all the raw data. All authors read and approved the final manuscript.

Ethics approval and consent to participate

The patients in the present study provided written informed consent. The present study was designed in accordance with The Declaration of Helsinki and approved by the ethics committee of Sanbo Brain Hospital, Capital Medical University (approval no. SBNK-YJ-2020-014-01).

Patient consent for publication

Not applicable.

Competing interests

The authors declare that they have no competing interests.

References

1. Müller H, Merchant T, Warmuth-Metz M, Martinez-Barbera J and Puget S: Craniopharyngioma. Nat Rev Dis Primers 5: 75, 2019.
2. Louis DN, Perry A, Reifenberger G, von Deimling A, Figarella-Branger D, Cavenee WK, Ohgaki H, Wiestler OD, Kleihues P and Ellison DW: The 2016 World Health Organization classification of tumors of the central nervous system: A summary. Acta Neuropathol 131: 803-820, 2016.
3. Martinez-Barbera J: Molecular and cellular pathogenesis of adamantinomatous craniopharyngioma. Neuropathol Appl Neurobiol 41: 721-732, 2015.
4. Whelan R, Prince E, Gilani A and Hankinson T: The inflammatory milieu of adamantinomatous craniopharyngioma and its implications for treatment. J Clin Med 9: 519, 2020.
5. Wang S, Song R, Wang Z, Jing Z, Wang S and Ma J: S100A8/A9 in inflammation. Front Immunol 9: 1298, 2018.
6. Martinsson H, Yhr M and Enerbäck C: Expression patterns of S100A7 (psoriasin) and S100A9 (calgranulin-B) in keratinocyte differentiation. Exp Dermatol 14: 161-168, 2005.
7. Christmann C, Zenker S, Martens L, Hübner J, Loser K, Vogl T and Roth J: Interleukin 17 promotes expression of alarmins S100A8 and S100A9 during the inflammatory response of keratinocytes. Front Immunol 11: 599947, 2021.
8. Mischke D, Korge BP, Marenholz I, Volz A and Ziegler A: Genes encoding structural proteins of epidermal cornification and S100 calcium-binding proteins form a gene complex ('epidermal differentiation complex') on human chromosome 1q21. J Invest Dermatol 106: 989-992, 1996.
9. Argyris PP, Slama Z, Malz C, Koutlas IG, Pakzad B, Patel K, Kademani D, Khammanivong A and Herzberg MC: Intracellular calprotectin (S100A8/A9) controls epithelial differentiation and caspase-mediated cleavage of EGFR in head and neck squamous cell carcinoma. Oral Oncol 95: 1-10, 2019.
10. Lin D, Wang Y, Zhou Z and Lin Z: Immune microenvironment of primary and recurrent craniopharyngiomas: A study of the differences and clinical significance. World Neurosurg 127: e212-e220, 2019.
11. Rakha E, Puls F, Saidul I and Furness P: Torsion of the testicular appendix: Importance of associated acute inflammation. J Clin Pathol 59: 831-834, 2006.
12. Vidal AP, Andrade BM, Vaisman F, Cazarin J, Pinto LF, Breitenbach MM, Corbo R, Caroli-Bottino A, Soares F, Vaisman M and Carvalho DP: AMP-activated protein kinase signaling is upregulated in papillary thyroid cancer. Eur J Endocrinol 169: 521-528, 2013.
13. Han SA, Jang JH, Won KY, Lim SJ and Song JY: Prognostic value of putative cancer stem cell markers (CD24, CD44, CD133, and ALDH1) in human papillary thyroid carcinoma. Pathol Res Pract 213: 956-963, 2017.
14. Kusama K, Katayama Y, Oba K, Ishige T, Kebusa Y, Okazawa J, Fukushima T and Yoshino A: Expression of hard alpha-keratins in pilomatrixoma, craniopharyngioma, and calcifying odontogenic cyst. Am J Clin pathol 123: 376-381, 2005.
15. Wang CH, Qi ST, Fan J, Pan J, Peng JX, Nie J, Bao Y, Liu YW, Zhang X and Liu Y: Identification of tumor stem-like cells in admanatimomatous craniopharyngioma and determination of these cells' pathological significance. J Neurosurg: 1-11, 2019 (Epub ahead of print).
16. Andoniadou CL, Gaston-Massuet C, Reddy R, Schneider RP, Blasco MA, Le Tissier P, Jacques TS, Pevny LH, Dattani MT and Martinez-Barbera JP: Identification of novel pathways involved in the pathogenesis of human adamantinomatous craniopharyngioma. Acta Neuropathol 124: 259-271, 2012.
17. Andoniadou CL, Matsushima D, Mousavy Gharavy SN, Signore M, Mackintosh AI, Schaeffer M, Gaston-Massuet C, Mollard P, Jacques TS, Le Tissier P, *et al*: Sox2(+) stem/progenitor cells in the adult mouse pituitary support organ homeostasis and have tumor-inducing potential. Cell Stem Cell 13: 433-445, 2013.
18. Cmoch A, Groves P, Palczewska M and Pikuła S: S100A proteins in propagation of a calcium signal in norm and pathology. Postepy Biochem 58: 429-436, 2012.
19. Fuellen G, Foell D, Nacken W, Sorg C and Kerkhoff C: Absence of S100A12 in mouse: Implications for RAGE-S100A12 interaction. Trends Immunol 24: 622-624, 2003.
20. Apps JR, Carreno G, Gonzalez-Meljem JM, Haston S, Guiho R, Cooper JE, Manshaei S, Jani N, Hölsken A, Pettorini B, *et al*: Tumour compartment transcriptomics demonstrates the activation of inflammatory and odontogenic programmes in human adamantinomatous craniopharyngioma and identifies the MAPK/ERK pathway as a novel therapeutic target. Acta Neuropathol 135: 757-777, 2018.
21. Pettorini BL, Inzitari R, Massimi L, Tamburrini G, Caldarelli M, Fanali C, Cabras T, Messana I, Castagnola M and Rocco C: The role of inflammation in the genesis of the cystic component of craniopharyngiomas. Childs Nerv Syst 26: 1779-1784, 2010.
22. Desiderio C, Martelli C, Rossetti DV, Di Rocco C, D'Angelo L, Caldarelli M, Tamburrini G, Iavarone F, Castagnola M, Messana I, *et al*: Identification of thymosins β4 and β 10 in paediatric craniopharyngioma cystic fluid. Childs Nerv Syst 29: 951-960, 2013.
23. Gong J, Zhang H, Xing S, Li C, Ma Z, Jia G and Hu W: High expression levels of CXCL12 and CXCR4 predict recurrence of adamanti-nomatous craniopharyngiomas in children. Cancer Biomark 14: 241-251, 2014.
24. Coy S, Rashid R, Lin JR, Du Z, Donson AM, Hankinson TC, Foreman NK, Manley PE, Kieran MW, Reardon DA, *et al*: Multiplexed immunofluorescence reveals potential PD-1/PD-L1 pathway vulnerabilities in craniopharyngioma. Neuro Oncol 20: 1101-1112, 2018.
25. Sprenkeler EGG, Zandstra J, van Kleef ND, Goetschalckx I, Verstegen B, Aarts CEM, Janssen H, Tool ATJ, van Mierlo G, van Bruggen R, *et al*: S100A8/A9 is a marker for the release of neutrophil extracellular traps and induces neutrophil activation. Cells 11: 236, 2022.
26. Mihaila AC, Ciortan L, Macarie RD, Vadana M, Cecoltan S, Preda MB, Hudita A, Gan AM, Jakobsson G, Tucureanu MM, *et al*: Transcriptional profiling and functional analysis of N1/N2 neutrophils reveal an immunomodulatory effect of S100A9-blockade on the pro-inflammatory N1 subpopulation. Front Immunol 12: 708770, 2021.
27. Vogl T, Tenbrock K, Ludwig S, Leukert N, Ehrhardt C, van Zoelen MA, Nacken W, Foell D, van der Poll T, Sorg C and Roth J: Mrp8 and Mrp14 are endogenous activators of Toll-like receptor 4, promoting lethal, endotoxin-induced shock. Nat Med 13: 1042-1049, 2007.
28. Shichita T, Ito M, Morita R, Komai K, Noguchi Y, Ooboshi H, Koshida R, Takahashi S, Kodama T and Yoshimura A: MAFB prevents excess inflammation after ischemic stroke by accelerating clearance of damage signals through MSR1. Nat Med 23: 723-732, 2017.
29. Sreejit G, Abdel-Latif A, Athmanathan B, Annabathula R, Dhyani A, Noothi SK, Quaife-Ryan GA, Al-Sharea A, Pernes G, Dragoljevic D, *et al*: Neutrophil-derived S100A8/A9 amplify granulopoiesis after myocardial infarction. Circulation 141: 1080-1094, 2020.
30. Mohr T, Zwick A, Hans MC, Bley IA, Braun FL, Khalmurzaev O, Matveev VB, Loertzer P, Pryalukhin A, Hartmann A, *et al*: The prominent role of the S100A8/S100A9-CD147 axis in the progression of penile cancer. Front Oncol 12: 891511, 2022.
31. Li HB, Wang JL, Jin XD, Zhao L, Ye HL, Kuang YB, Ma Y, Jiang XY and Yu ZY: Comprehensive analysis of the transcriptional expressions and prognostic value of S100A family in pancreatic ductal adenocarcinoma. BMC Cancer 21: 1039,2021.
32. Lukanidin E and Sleeman JP: Building the niche: The role of the S100 proteins in metastatic growth. Semin Cancer Biol 22: 216-225, 2012.
33. Liu Y, Kosaka A, Ikeura M, Kohanbash G, Fellows-Mayle W, Snyder LA and Okada H: Premetastatic soil and prevention of breast cancer brain metastasis. Neuro Oncol 15: 891-903, 2013.
34. Gaston-Massuet C, Andoniadou CL, Signore M, Jayakody SA, Charolidi N, Kyeyune R, Vernay B, Jacques TS, Taketo MM, Le Tissier P, *et al*: Increased Wingless (Wnt) signaling in pituitary progenitor/stem cells gives rise to pituitary tumors in mice and humans. Proc Nati Acad Sci USA 108: 11482-11487, 2011.